Robotica (2006) volume 24, pp. 365–372. © 2006 Cambridge University Press
doi:10.1017/S0263574705002286 Printed in the United Kingdom

Simple two degree of freedom structures and their properties

Rafael Osypiuk*, Bernd Finkemeyer† and Stanislaw Skoczowski*

(Received in Final Form: September 3, 2005, first published online 24 February 2006)

SUMMARY

A two-degree of freedom control system that is most frequently encountered in practice is the so-called Internal Model Control (IMC) structure. However, the design procedure of such a structure does not present an easy task, which implies a limited utility of IMC. In this paper two alternative solutions are proposed that may be lumped together as Model-Following Control (MFC). These are two-loop control systems being easy to implement and offering interesting properties. Theoretical assumptions have been verified experimentally on a two-joint robot manipulator. Both qualitative and quantitative results yielded by experiments are presented and discussed.

KEYWORDS: IMC structure; Control system; Model-following control.

I. INTRODUCTION

The classic single-loop feedback structure is currently encountered in almost 95% of industrial applications.[1] However, there are challenges, of which robotics is an example, where the classic single-loop structure is unable to cope with satisfactorily. The robot manipulator represents a control plant, which is both nonlinear and time-variant. To ensure the required control performance, employing a more complicated control structure here may be found to be necessary. If the dynamic process model is available, then model-based control systems (MBC) may be of use.[2] An example is the well-known Internal Model Control (IMC) with one or two degrees of freedom, which allows a more effective pole placement (Fig. 1).

The main problem that comes up with the use of IMC consists in finding the compensator $C(s)$. To solve the problem, a recourse to optimisation theory is often necessary.[3] This is a much more difficult task than tuning a classic PID controller. Additionally, if the plant is perturbed, the IMC system may yield questionable results in contrast to classic control systems.

To obviate the difficulties two solutions were proposed, both based on 2DOF IMC, where an additional feedback path makes sure that the drawbacks mentioned are eliminated. The proposed solutions are designated as MFC-m (model feedback)[4–9] and MFC-p (plant feedback),[8] also called MFC/IMC. They are noted for their robustness and ease in implementation.

* Institute of Control Engineering, Technical University of Szczecin, ul. 26 Kwietnia 10, 70-313 Szczecin (Poland).
† Institute for Robotics and Process Control, Technical University of Braunschweig, Mühlenpfordtstr. 23, 38106 Braunschweig (Germany). E-mail: b.finkemeyer@tu-bs.de
Corresponding author. Bernd Finkemeyer. E-mail: b.finkemeyer@tu-bs.de

II. ESSENTIAL PROPERTIES OF THE PROPOSED MFC-M AND MFC-P STRUCTURES

Model-Following Control (MFC) represents a relatively novel concept, hence being little popular, in comparison to such control structures as: feedforward, conditional feedback or IMC. Although the notion of MFC is frequently encountered in publications, it is uncommon for them to deal with a two-loop structure shown in Fig. 2.

The structure of Fig. 2 looks similar to that of 2DOF IMC. The difference consists in adding an additional feedback path that embraces the plant model $M(s)$. This causes the $C(s)$ compensator in 2DOF IMC (Fig. 1) to become a model controller $R_m(s)$ in MFC-m. Such an approach relieves the system designer of having to find the inverse model of the plant, which is a significant drawback to IMC. On the other hand, the approach requires determining the structure and parameters of the $R_m(s)$ controller, which presents a simple and classic task.

Assuming the system of Fig. 2 is subject to disturbances $z(s)$, its output is given by

$$y_{MFC-m} = \frac{R_m P(1 + R_k M)}{1 + R_m M + R_k P + R_m R_k M P} y_0 + \ldots \\ \ldots + \underbrace{\frac{1}{1 + R_k P}}_{S_m(s)} z \qquad (1)$$

As may be noted, if $P(s) = M(s)$, the system output tracks ideally the model output, which makes it possible to tune the corrective controller $R_k(s)$ with respect to the amplitude and frequency of disturbances $z(s)$. If $z(s) = 0$, the same simplification will be obtained for $R_m(s) = R_k(s)$, however in this case the MFC-m system is reduced to a single-loop system. In order to circumvent this and make use of advantages offered by the structure of Fig. 2, the following condition should be fulfilled:[8]

$$|R_k(j\omega)| > |R_m(j\omega)| \quad \text{for} \quad \omega \in [0, \infty) \qquad (2)$$

In the MFC-m system two loops may be distinguished, of which the first one is an entirely independent model loop. The loop is unable to "see" both the process itself and disturbances acting on it. This can be changed by introducing a system output $y(s)$ driven feedback in the first loop, instead of a model output $y_m(s)$ driven one, as it takes place in the

https://doi.org/10.1017/S0263574705002286 Published online by Cambridge University Press

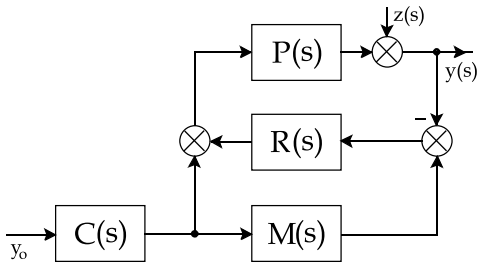


Fig. 1. Structure of the 2DOF IMC system.

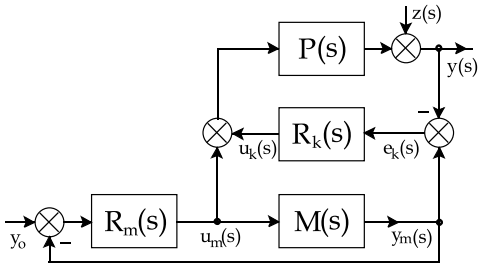


Fig. 2. Structure of the MFC-m system.

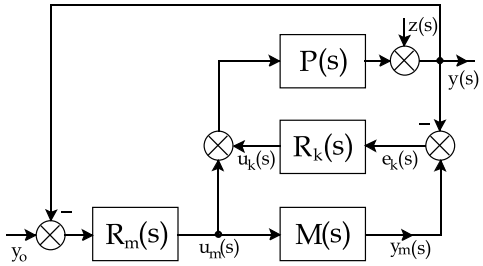


Fig. 3. Structure of the MFC-p system.

MFC-m system. Such a modification leads to a system with new interesting properties, which is referred to as MFC-p (Fig. 3).[9]

In the case of the MFC-m system the model loop works out the main control constituent $u_m(s)$. On the other hand, in tracking the $y_m(s)$ the corrective loop output compensates any model inaccuracies and the effect produced by system disturbances $z(s)$. Such a clear division of tasks visible in the MFC-m structure is not so obvious when the modified MFC-p one is considered. As may be noted, the model controller $R_m(s)$ in the MFC-p system is driven by the process error, which provides an active participation of both controllers in the process control. As it will be shown later, this circumstance has a substantial effect on the system robustness. The MFC-p output is given by

$$y_{MFC-p} = \frac{R_m P(1 + R_k M)}{1 + R_m P + R_k P + R_m R_k M P} y_0 + \ldots$$
$$\ldots + \underbrace{\frac{1}{1 + R_m P + R_k P + R_m R_k M P}}_{S_p(s)} z \quad (3)$$

When eq. 3 is compared with eq. 1, it may be noted that the disturbance sensitivity $S_p(s)$ of MFC-p is lower than that of MFC-m $S_m(s)$, and, in addition, the both structures differ

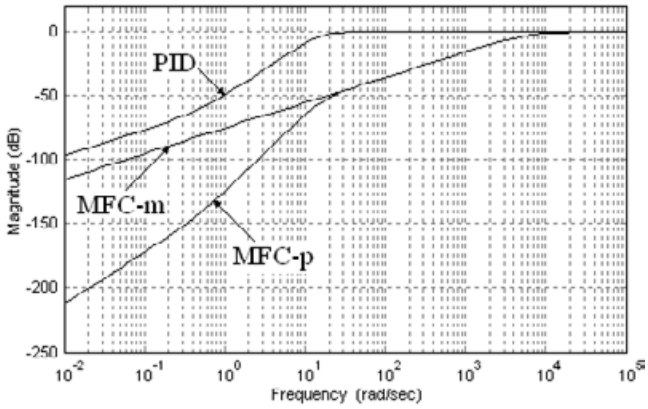


Fig. 4. Damping of system disturbances z(s) provided by the single-loop PID structure and the MFC ones.

in stability conditions. The lower sensitivity of MFC-p is illustrated in Fig. 4, where the frequency response for the classic PID structure is also plotted for comparison (both process parameters and controller settings are the same in each case here).

III. ROBUSTNESS

Besides the relative sensitivity,[5] the system robustness defined as the ability to preserve the system stability at occurring process perturbations is also taken into account here. Process perturbations may be modelled in several ways.[10] If $M(s)$ is the nominal model of the actual process $K(s)$, then a multiplicative uncertainty model (viewed from the output), also called relative error,[5] is defined by

$$K = M + \Delta_m M = (1 + \Delta_m) M \quad (4)$$

To determine the robustness of the MFC structures use was made of a condition to preserve stability in a single-loop PID system in the presence of a multiplicative perturbation acting on the plant output.[10] In doing this, the two-loop MFC systems have been reduced to the classic structure (of course, observing stability conditions), and, consequently, the desired sensitivity has been found by analogy.

Transfer function of the perturbed MFC-m system is simplified to classic form. In Fig. 5 y'_{0m} is defined by

$$y'_{0m} = y_0 \frac{1 + R_k M}{1 + R_m M} \quad (5)$$

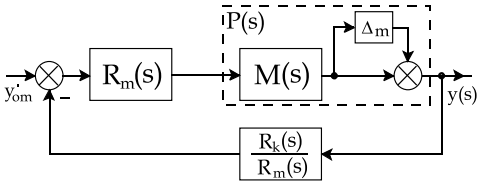


Fig. 5. Equivalent block diagram of the MFC-m system for the purpose of sensitivity analysis.

https://doi.org/10.1017/S0263574705002286 Published online by Cambridge University Press

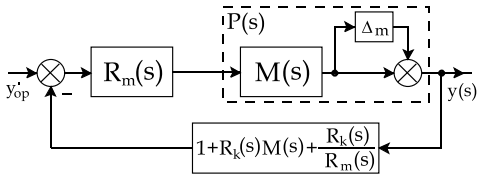


Fig. 6. Equivalent block diagram of the MFC-p system for the purpose of sensitivity analysis.

Similarly, for MFC-p we get the corresponding block diagram of Fig. 6. There, y'_{0p} is defined by

$$y'_{0p} = y_0(1 + R_k M) \tag{6}$$

If we assume that both the perturbation Δ_m and the nominal control system are asymptotically stable, then the necessary and sufficient condition for the perturbed system to be asymptotically stable is given by the following inequalities: for MFC-m:[8]

$$|\Delta_m|_{MFC-m} < \frac{|1 + MR_k|}{|MR_m|} = |T_m| \tag{7}$$

for MFC-p:

$$|\Delta_m|_{MFC-p} < \frac{|(1 + MR_m)(1 + MR_k)|}{|MR_m|} = \ldots \tag{8}$$
$$\ldots = |T_m||(1 + MR_m)|$$

For comparison, the analogous stability condition for the perturbed classic single-loop PID structure is defined by reference [2]:

$$|\Delta_m|_{PID} < \frac{|1 + MR_m|}{|MR_m|} \tag{9}$$

As follows from eq. (9), in order to get big values of $|\Delta_m(s)|$, the right-hand side of the inequality (9) should be as great as possible. This is connected with lowering the gain of the controller, hence, with "slowing down" of its action. Unfortunately, as a result the reference signal tracking by the controlled variable is impaired, and the effect of disturbances $z(s)$ is less damped.

When eq. (9) is compared with eq. (7), a clear difference in robustness of both structures may be noted. The condition (7) is fulfilled the more, the stronger is the inequality

$$|R_k| > |R_m|. \tag{10}$$

Hence, the greater is the gain of the corrective controller $R_k(s)$, the greater is the robustness exhibited by the MFC-m structure without tracking the reference and damping system disturbances (eq. (1)) having been impaired. Of greater robustness is the MFC-p system, which is exhibited by the inequality (8). Here the allowable uncertainty $|\Delta_m(s)|$ is $|1 + M(s)R_m(s)|$ times greater than that provided by the MFC-m structure. In Fig. 7 results of simulation tests for robustness carried out on both MFC systems, and the classic

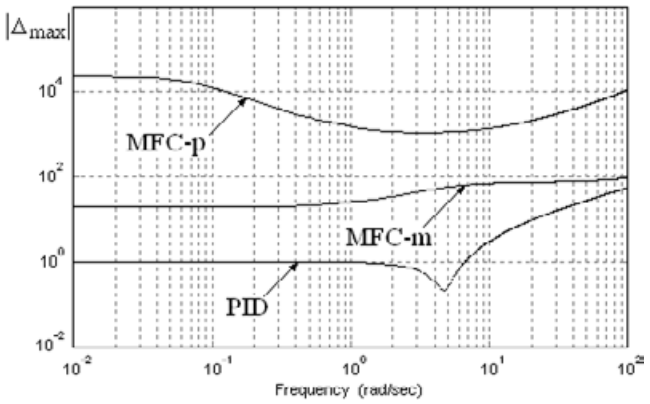


Fig. 7. Allowable values of perturbations $\Delta_m(s)$ for control structures under consideration.

PID structure are depicted. The robustness offered may be read off here from the logarithmic ordinate axis.

IV. STABILITY

In general, the system to be designed should be as less sensitive to disturbances caused by changes in inputs, or initial values, or system parameters, as possible.[5] To assess the stability of MFC systems the approach based on analysis of roots of the characteristic equation is employed. The following system of equations holds for the both MFC structures:

$$\begin{aligned} y &= Pu \\ u &= u_m + R_k e_k \\ e_k &= y_m - y \end{aligned} \tag{11}$$

where the model output $y_m(s)$ is defined depending on the structure considered:

$$y_{m(MFC-m)} = (y_0 - y_m)MR_m = y_0 \frac{R_m M}{1 + R_m M} \tag{12}$$

$$y_{m(MFC-p)} = (y_0 - y)MR_m \tag{13}$$

From (11) the corrective error e_k both for MFC-m and MFC-p structures is defined by

$$e_k = \frac{u_m(M - P)}{1 + R_k P} \tag{14}$$

where, in view of eqs. (12) and (13), $u_m(s)$ depends on the corresponding MFC structure. Let the elements of eq. (14) be given in a rational form

$$u_m = \frac{l_u}{m_u}, R_k = \frac{l_r}{m_r}, M = \frac{l_m}{m_m}, P = \frac{l_p}{m_p} \tag{15}$$

Substituting (15) into (14) yields in

$$e_k = \frac{l_u m_r (l_m m_p - l_p m_m)}{m_u m_m (m_r m_p + l_r l_p)} \tag{16}$$

https://doi.org/10.1017/S0263574705002286 Published online by Cambridge University Press

The sought-for characteristic equation of MFC systems under analysis is obtained by setting the denominator of (16) equal to zero. This equation presents the only source of information about necessary conditions for the system under study to be stable. As follows from (16), the MFC structures are stable if the polynomials $m_u(s)$, $m_m(s)$ and $(m_r m_p + l_r l_p)$ are Hurwitz ones, i.e. their poles have negative real parts. This means that stability is demanded not only from the process loop, but also from the model $M(s)$ itself, and its manipulated variable $u_m(s)$. In the case of MFC-m the model $M(s)$ is controlled in an independent classic feedback loop by

$$u_{m(MFC-m)} = y_0 \frac{R_m}{1 + R_m M} \tag{17}$$

That is why, the stability of the MFC-m structure is strictly connected with the stability of the single-loop system.

In the case of MFC-p, the situation is much more complicated, since the both loops are mutually dependent in both directions. Hence, the stability of $u_m(s)$ depends on the stability of $u_k(s)$ and vice versa. So $u_m(s)$ is a function of $u_k(s)$:

$$u_{(MFC-p)} = \frac{R_m(y_0 - P u_k)}{1 + R_m P} \tag{18}$$

As may be seen from (17), the necessary condition for the MFC-m structure to be stable is that the model loop $R_m(s)M(s)$ and the process loop $R_k(s)P(s)$ are both stable together with the model $M(s)$. For the MFC-p to be stable, the stability of loops $R_k(s)P(s)$ and $R_m(s)P(s)$ along with the stability of the model $M(s)$ is required (eq. (18)).

V. MODELLING AND IMPLEMENTATION OF MFC ALGORITHMS

The proposed two-loop control systems have been tested in experiments with the two-joint serial robot manipulator EDDA (Experimental Direct Drive Arm) as control plant. In order for MFC to be implemented, a dynamic plant model is necessary. Since modelling of kinematic chains is widely reflected in the literature,[11,12] only general information about it is given below.

There are two known methods to model dynamics of a manipulator, namely the iterative Newton-Euler method and the energy-based Lagrange method. Of course, both approaches yield in the same result, i.e. the dynamic inverse process model. However, it should be noted that MFC systems are based on the forward model of the process to be controlled. Therefore, the model of the manipulator need to be inversed, which is possible if conditions for mass matrix $\mathbf{M}(\mathbf{q})$ invertibility are satisfied. Thus, the forward model of the kinematic chain with viscosous friction can be written as:

$$\ddot{\mathbf{q}} = \mathbf{M}^{-1}(\mathbf{q})[\tau - \mathbf{C}(\mathbf{q}, \dot{\mathbf{q}}) - \mathbf{G}(\mathbf{q}) - \mathbf{F}(\dot{\mathbf{q}})] \tag{19}$$

where $\mathbf{M}$ is the $n \times n$ manipulator inertia matrix, $\mathbf{C}$ is the $n \times n$ matrix of velocity effect (centrifugal and Coriolis torques), $\mathbf{G}$ is the $n \times 1$ vector of gravitational torque, $\mathbf{F}$ is the $n \times 1$ vector of friction force, τ is the $n \times 1$ vector of joint torque, $\mathbf{q}$, $\dot{\mathbf{q}}$, and $\ddot{\mathbf{q}}$ are the $n \times 1$ vectors of the joint displacement, velocity and acceleration terms, respectively. As may be inferred from (19), in order to find acceleration for individual manipulator joints, the knowledge of their velocities and positions is needed. The lacking state variables can be found through double integration of each term.[11] Employing MATLAB/Simulink and its advanced real-time workshop (RTW)in combination with RT-Opal, a software which enables the execution of Simulink models on a QNX-PC, made it possible to implement the investigated control structures in an easy way. The experimental setup with its basic components is depicted below in Fig. 8.

EDDA is driven by NSK-manufactured high-torque reluctance motors equipped with NSK Control Unit. The terminal enables the operation mode of the Control Unit to be selected (in our experiment a direct access to torques has been chosen). The Control Unit is connected to a Vigilant-manufactured I/O card, which delivers torques for individual motors, besides giving access to the current position of joints. This card, for the lack of a signal processor, requires a separate PC together with the operation system QNX. The computer, in its turn, communicates through a TCP/IP channel with another PC equipped with Windows NT, where the mentioned MATLAB software and RT-Opal are running. Files generated by RTW are delivered to the QNX system. There they are compiled and are ready to execute. They can be online parameterised by RT-Opal.



Fig. 8. Experimental setup.

https://doi.org/10.1017/S0263574705002286 Published online by Cambridge University Press

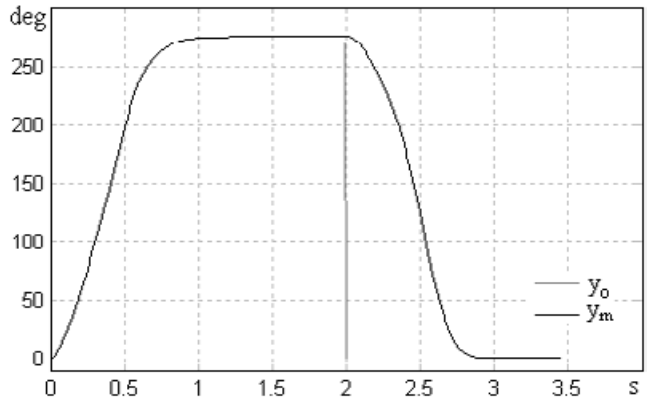


Fig. 9. Model controller tuning by way of simulation (Joint 2). Effect of strong static nonlinearities exhibited by the model (19).

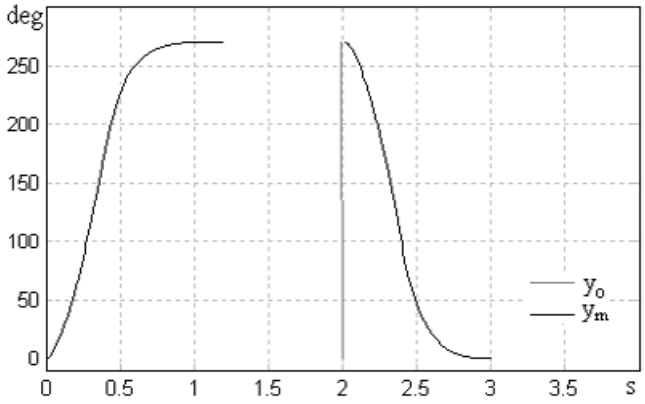


Fig. 10. Model controller tuning by way of simulation (Joint 2). Improving the control performance of the model after its static nonlinearities having been reduced (20).

VI. EXPERIMENTAL RESULTS

Once the dynamic system model is available, and the MFC structure is implemented, the controllers may be tuned. If the corrective controller $R_k(s)$ requires to be tuned online, then the model controller $R_m(s)$ settings may be chosen, for example, by way of simulation. However, it should be noted that in the case of MFC-p the model controller also "sees" the system disturbances $z(s)$, the nature of which should be taken into account when tuning. This problem is purposely omitted here in order to notice the effect of the system structure on control performance at identical MFC system parameters.

For the both MFC systems the model controller $R_m(s)$ settings are chosen in a single-loop structure. To maintain the demanded control performance for the plant output $y(s)$, also the model output $y_m(s)$ has to show the required performance. Since the classic single-loop PID system exhibits limited robustness only, it may be necessary to simplify the process model to a form that ensures the required time responses. The problem appears if the manipulator is controlled in a single-loop structure, where ensuring satisfactory control performance in each working point is impossible to achieve due to strong static nonlinearities exhibited (Fig. 9).

The effect of controller integration time on control performance has been discussed in reference [7]. Since finding compromise controller settings for the entire working area of the manipulator is fraught with great difficulties, the model has been simplified by the effect of gravitation **G**. Hence, the model eventually adopted for control purposes assumes the form:

$$\ddot{\mathbf{q}} = \mathbf{M}^{-1}(\mathbf{q})[\tau - \mathbf{C}(\mathbf{q}, \dot{\mathbf{q}}) - \mathbf{F}(\dot{\mathbf{q}})] \tag{20}$$

Thus, the simplified model ensures an aperiodic output $y_m(s)$ not affected by a steady-state error, which is depicted in Fig. 10.

After the model loop was parameterised, the corrective controller $R_k(s)$ has been tuned experimentally. It is essential to point out, that settings for both MFC structures were chosen only once, and they did not differ from each other. Results of actual control obtained for the same set-point change are given below. In the case considered the first joint should remain in a standstill when the second joint changes its position from 0° to 90°. Because of strong dynamic couplings keeping the first joint in a standstill is impossible (Fig. 11). As may be seen, this phenomenon occurs already in the model loop; therefore, a better control performance in the process loop cannot be expected. For the second joint, however, the desired aperiodic transient response has been obtained, though affected by a steady-state error of several degrees (Fig. 12).

In spite of strong integrating properties, the corrective controller $R_k(s)$ is unable to cope with static nonlinearities exhibited by the manipulator. Hence, wherever the effect of

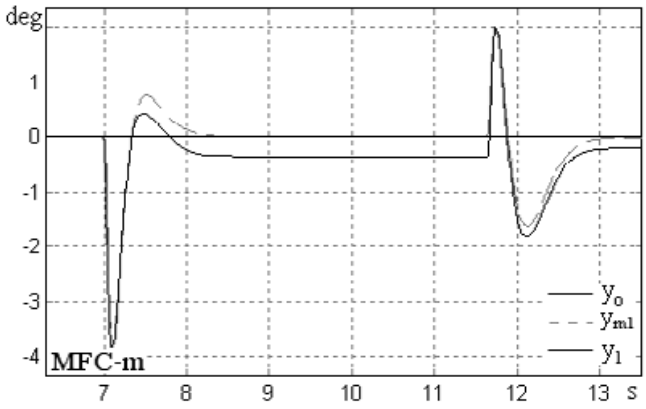


Fig. 11. Control results delivered by the actual MFC-m in the case of the first joint (effect of dynamic couplings).

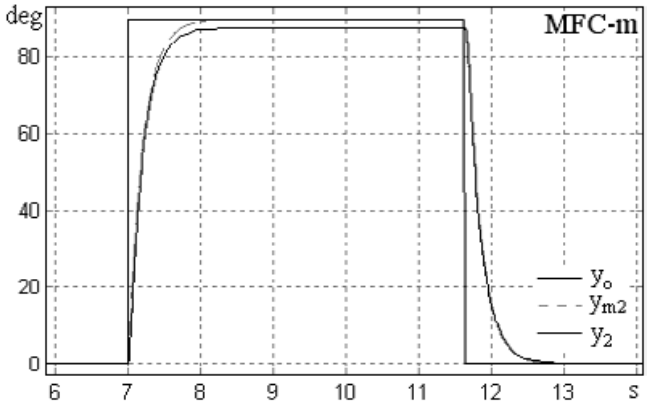


Fig. 12. Control results delivered by the actual MFC-m in the case of the second joint.

https://doi.org/10.1017/S0263574705002286 Published online by Cambridge University Press

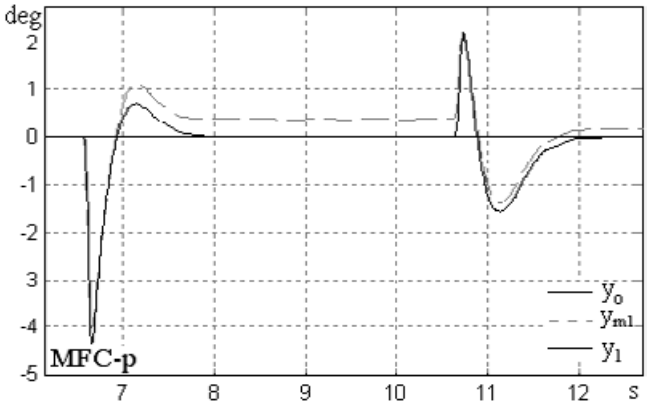


Fig. 13. Control results delivered by the actual MFC-p in the case of the first joint (effect of dynamic couplings).

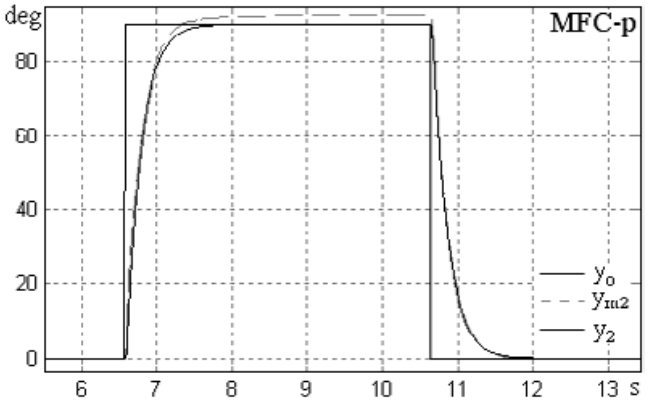


Fig. 14. Control results delivered by the actual MFC-p in the case of the second joint.

gravitation or dynamic couplings requires that a constant torque be generated, a distinct steady-state error appears in the MFC-m structure. This adverse effect can be avoided by employing an additional compensator (inverse gravitational model) in the first loop of MFC-m[6] or by supplementing the two-loop structure by a next loop to compensate the nonlinear effect of gravitation.[7]

To eliminate the steady-state error and maintain the system simplicity at the same time, a minor modification of the two-loop structure leading to the MFC-p one will suffice. As may be seen in Figs. 13 and 14, the plant output in steady-state tracks ideally the reference signal. Only the model output $y_m(s)$ is affected by the steady-state error, which is caused by the manipulated variable $u_m(s)$ created from the plant output, but applied simultaneously to the model, where the acceleration of gravity is disregarded (20). Such a good control performance offered by MFC-p results from 'active' participation of both controllers in the process control.

EDDA has a joint with a variable centre of gravity (Fig. 15), which facilitates testing the robustness of control algorithms. This peculiarity was utilized in the next experiment, where the control performance was measured for two extreme points of mass m (the controllers were tuned nominally for the mass m being positioned at the centre of the joint). This time the second joint had to remain in a standstill with the first joint changing its position from 0° to 90°. Since different mass positioning influenced only the steady-state error exhibited



Fig. 15. The way the centre of gravity of the second joint is changed.

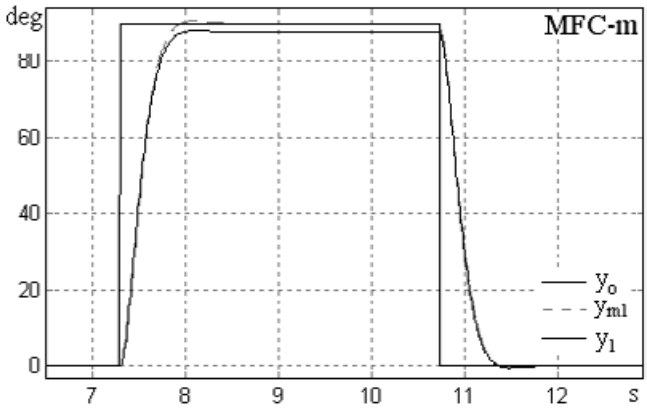


Fig. 16. Control results delivered by MFC-m for the first joint after the centre of gravity of the second joint had been changed.

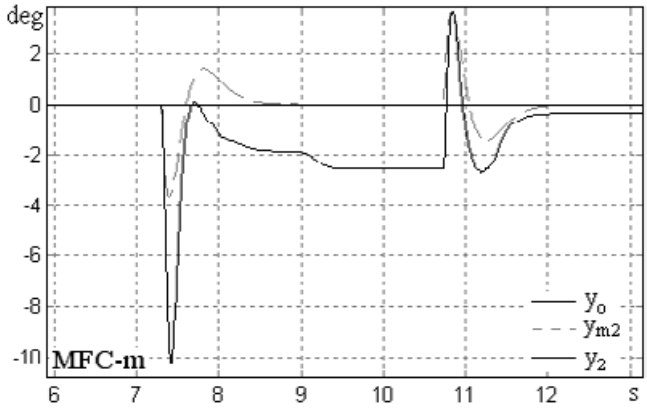


Fig. 17. Control results delivered by MFC-m for the second joint with its centre of gravity having been changed.

by the MFC-m structure, below there are presented only those time responses where the mass m was most distant from the centre of rotation of the joint.

Whereas the change in plant parameters affects the steady-state error (Figs. 16 and 17) in the case of MFC-m, the control performance remains unaffected in the case of MFC-p. We can only notice the effect of process perturbation on the model output (Fig. 19). Obviously, this is caused by a change in the manipulated variable $u_m(s)$ fitted to the plant perturbed. It should be mentioned here that a comparison between the MFC-m structure and the classic PID one has been drawn in reference [6]. As it turned out, the single-loop structure was unable to provide stability in the whole EDDA's working area.

https://doi.org/10.1017/S0263574705002286 Published online by Cambridge University Press

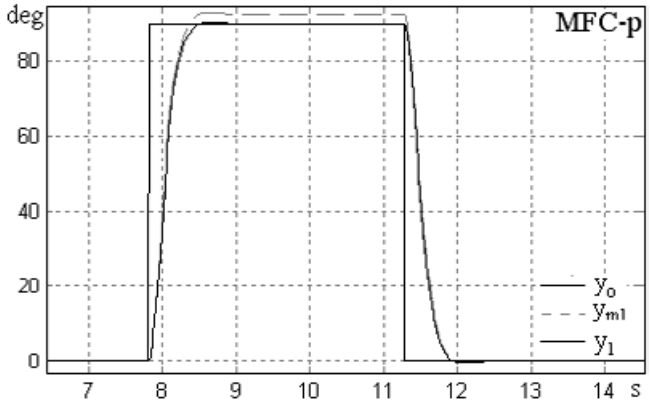


Fig. 18. Control results delivered by MFC-p for the first joint after the centre of gravity of the second joint had been changed.

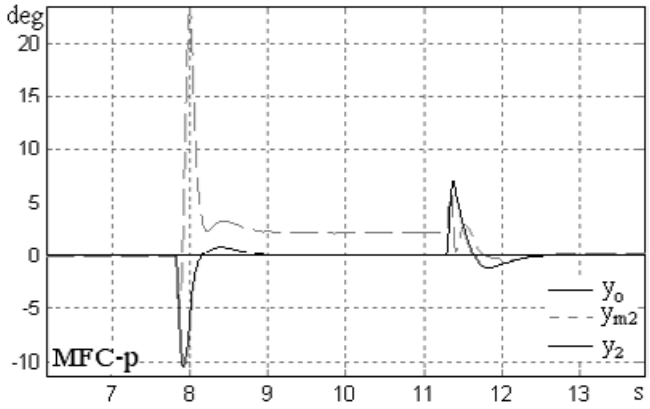


Fig. 19. Control results delivered by MFC-p for the second joint with its centre of gravity having been changed.

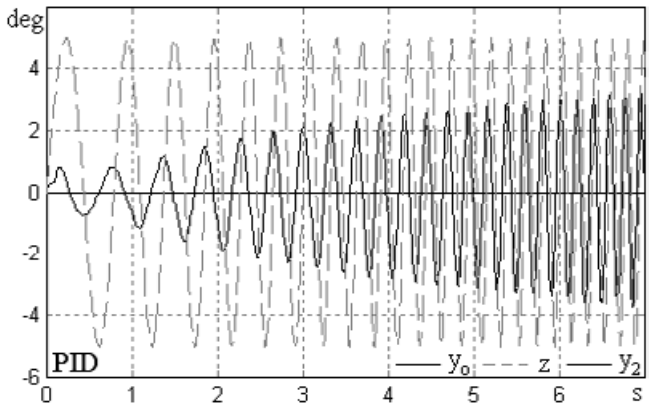


Fig. 20. Suppression of system disturbances z(s) in the case of the classic single-loop PID structure.

Since any modelling inaccuracies may be represented by system disturbances $z(s)$,[12] therefore it is important to analyse the control system ability to suppress those. In doing this, a test has been carried out where a sinusoidal disturbance was applied to the output of the second joint for the three control systems under comparison (Fig. 18). As may be noted, the results (Figs. 20–22) obtained check well with theoretical predictions (Fig. 4).

To assess suppression of system disturbances not only qualitatively, but also quantitatively, integral performance

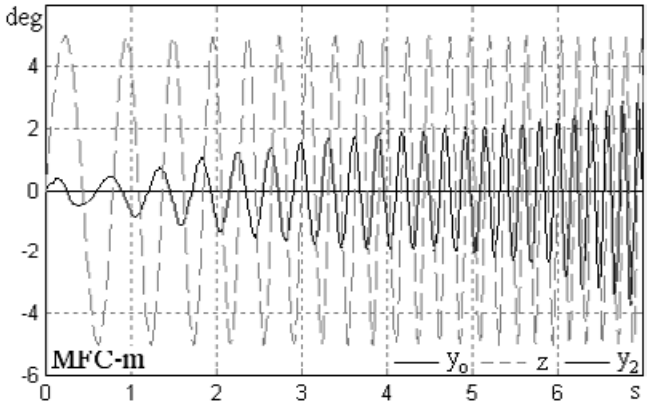


Fig. 21. Suppression of system disturbances z(s) in the case of the MFC-m structure.

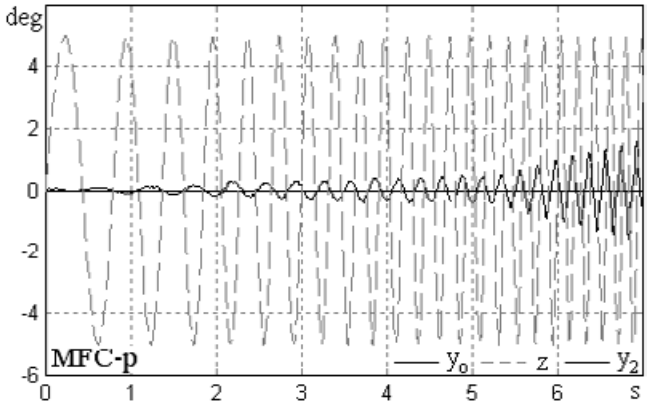


Fig. 22. Suppression of system disturbances z(s) in the case of the MFC-p structure.

Table I. Quantitative assessment of suppression of system disturbances made for the control structures under comparison.

	Integral criteria	
Structure	IAE (Integral of Absolute Errors)	ISE (Integral of Squared Errors)
PID	10.0	20.5
MFC-m	7.4	11.7
MFC-p	1.0	1.7

criteria have been used. The results obtained are summarized in Table I. The superiority of MFC-p over the other structures is readily apparent.

VII. CONCLUSIONS

The control structures presented in this paper are based on the forward process model. Since the number of control plants, for which finding their inverse models is actually possible, is very limited, the MFC systems present an interesting compromise between the classic PID control and IMC systems, or dissipative systems (e.g. those employing feedforward).

In reference [6] differences between a single-loop control system and a MFC-m one in the control of a real plant are discussed. Despite many advantages offered by MFC-m, its practical utility is limited due to complicated process

https://doi.org/10.1017/S0263574705002286 Published online by Cambridge University Press

models involved. This limitation has been eliminated through employing a multi-loop n-MFC structure[7] that corresponds intuitively to state-space control. The virtue of n-MFC is that there is no need for all process state variables to be available, hence, there is no need to use complicated estimators.

The tests carried out showed that strong process nonlinearities prevented achieving the demanded control performance for a MFC-m system. A minor modification introduced here led to the MFC-p system, which is characterized by significantly improved properties with respect to stability, robustness or suppression of system disturbances when compared to the original structure. Both MFC structures have been confronted with commonly used classic PID control structures. There exists a possibility to make MFC systems more insensitive to changes in process parameters or structure by employing H_∞ or fuzzy set approaches.

Acknowledgement

This research was supported by KBN (Polish State Committee for Scientific Research) under Grant No. 3 T11A 009 26 and by the German science foundation DFG.

References

1. K. J. Astroem and T. Haegglund, "The future of pid control. Special Issue on PID Control, Control Engineering Practice," *Journal of IFAC the International Federation of Automatic Control* **9**(11), 1163–1175 (2001).
2. P. Albertos, "Weighted model-based control," *European Control Conference ECC'93*, Netherlands (1993) pp. 1935–1939.
3. D. Schröder, *Elektrische Anriebe – Regelung von Antriebssystemen* (Springer, 2001).
4. G. Li, K. M. Tsang and S. L. Hos, "A novel model following scheme with simple structure for electrical position servo systems," *International Journal of Systems Science* **29**, 959–969 (1998).
5. G. Ludyk, *Theoritische Regelungste chnik* **2**. (Springer, 1995).
6. R. Osypiuk, B. Finkemeyer and F. M. Wahl, "Forward-model-based control system for robot manipulators," *Robotica* **22**(2), 155–161 (2004).
7. R. Osypiuk, B. Finkemeyer and F. M. Wahl, "Multi-loop model-based control structure for robot manipulators," *Robotica* **23** (4), 491–499 (2005).
8. S. Skoczowski, "Robust model following control with use of plant model," *International Journal of Systems Science* **32**(12), 1413–1427 (2005).
9. S. Skoczowski, "Struktury ukladow automatycznej regulacji oraz ich wlasciwosci odpornosciowe," *XIV Krajowa Konferencja Automatyki (2002)*, pages 24–27.
10. H. P. Geering, *Robuste Regelung* (Institut für Mess- uind Regeltechnik Eidgenössische Technische Hochschule, Zürich, 1999).
11. J. J. Craig, *Introduction to Robotics: Mechanics and Control* (Addison-Wesley Publishers Ltd., 1986).
12. M. W. Spong and M. Vidyasagar, *Robot Dynamics and Control* (John Wiley & Sons, New York, 1989).

https://doi.org/10.1017/S0263574705002286 Published online by Cambridge University Press